REFERENCES AND NOTES

1. C. B. Murray, D. J. Norris, M. G. Bawendi, *J. Am. Chem. Soc.* **115**, 8706–8715 (1993).
2. M. L. Landry, T. E. Morrell, T. K. Karagounis, C.-H. Hsia, C.-Y. Wang, *J. Chem. Educ.* **91**, 274–279 (2014).
3. I. L. Medintz, H. T. Uyeda, E. R. Goldman, H. Mattoussi, *Nat. Mater.* **4**, 435–446 (2005).
4. M. Bruchez Jr., M. Moronne, P. Gin, S. Weiss, A. P. Alivisatos, *Science* **281**, 2013–2016 (1998).
5. I. Gur, N. A. Fromer, M. L. Geier, A. P. Alivisatos, *Science* **310**, 462–465 (2005).
6. W. C. W. Chan, S. Nie, *Science* **281**, 2016–2018 (1998).
7. S. Coe, W.-K. Woo, M. Bawendi, V. Bulović, *Nature* **420**, 800–803 (2002).
8. V. L. Colvin, M. C. Schlamp, A. P. Alivisatos, *Nature* **370**, 354–357 (1994).
9. S. A. McDonald *et al.*, *Nat. Mater.* **4**, 138–142 (2005).
10. C. Burda, T. C. Green, S. Link, M. A. El-Sayed, *J. Phys. Chem. B* **103**, 1783–1788 (1999).
11. I. Robel, M. Kuno, P. V. Kamat, *J. Am. Chem. Soc.* **129**, 4136–4137 (2007).
12. K. E. Knowles, M. Malicki, E. A. Weiss, *J. Am. Chem. Soc.* **134**, 12470–12473 (2012).
13. R. Reisfeld, M. Gaft, T. Saridarov, G. Panczer, M. Zelner, *Mater. Lett.* **45**, 154–156 (2000).
14. M. Wojdak *et al.*, *Phys. Rev. B* **69**, 233315 (2004).
15. Z. Han, F. Qiu, R. Eisenberg, P. L. Holland, T. D. Krauss, *Science* **338**, 1321–1324 (2012).
16. K. Wu, Q. Li, Y. Du, Z. Chen, T. Lian, *Chem. Sci.* **6**, 1049–1054 (2015).
17. H. B. Yang *et al.*, *ACS Nano* **8**, 10403–10413 (2014).
18. E. Khon *et al.*, *Nano Lett.* **13**, 2016–2023 (2013).
19. M. Tabachnyk *et al.*, *Nat. Mater.* **13**, 1033–1038 (2014).
20. N. J. Thompson *et al.*, *Nat. Mater.* **13**, 1039–1043 (2014).
21. G. D. Scholes, *Adv. Funct. Mater.* **18**, 1157–1172 (2008).
22. A. L. Efros *et al.*, *Phys. Rev. B* **54**, 4843–4856 (1996).
23. M. Wu *et al.*, *Nat. Photon.* **10**, 31–34 (2016).
24. S. A. Crooker, T. Barrick, J. A. Hollingsworth, V. I. Klimov, *Appl. Phys. Lett.* **82**, 2793 (2003).
25. S. Hirayama, *J. Chem. Soc., Faraday Trans. I* **78**, 2411 (1982).
26. Y. Niko, Y. Hiroshige, S. Kawauchi, G. Konishi, *Tetrahedron* **68**, 6177–6185 (2012).
27. W. W. Yu, L. Qu, W. Guo, X. Peng, *Chem. Mater.* **15**, 2854–2860 (2003).
28. D. R. Baker, P. V. Kamat, *Langmuir* **26**, 11272–11276 (2010).
29. M. Montalti, A. Credi, L. Prodi, T. Gandolfi, *Handbook of Photochemistry* (CRC Press, Boca Raton, FL, ed. 3, 2006).
30. H. Zhu, Y. Yang, T. Lian, *Acc. Chem. Res.* **46**, 1270–1279 (2013).
31. J. M. Masnovi, E. A. Seddon, J. K. Kochi, *Can. J. Chem.* **62**, 2552–2559 (1984).
32. V. N. Soloviev, A. Eichhöfer, D. Fenske, U. Banin, *J. Am. Chem. Soc.* **123**, 2354–2364 (2001).
33. R. Bakalova, H. Ohba, Z. Zhelev, M. Ishikawa, Y. Baba, *Nat. Biotechnol.* **22**, 1360–1361 (2004).
34. E. I. Zenkevich *et al.*, *J. Phys. Chem. C* **115**, 21535–21545 (2011).
35. A. C. S. Samia, X. Chen, C. Burda, *J. Am. Chem. Soc.* **125**, 15736–15737 (2003).
36. T. N. Singh-Rachford, F. N. Castellano, *Inorg. Chem.* **48**, 2541–2548 (2009).
37. Z. Huang *et al.*, *Nano Lett.* **15**, 5552–5557 (2015).
38. Z. Huang *et al.*, *Chem. Mater.* **27**, 7503–7507 (2015).

ACKNOWLEDGMENTS

This work was supported by the Air Force Office of Scientific Research (grant FA9550-13-1-0106) and the Ultrafast Initiative of the U. S. Department of Energy, Office of Science, Office of Basic Energy Sciences, through Argonne National Laboratory under contract no. DE-AC02-06CH11357. M.Z. was supported by NSF (grant CHE-1465052).

SUPPLEMENTARY MATERIALS

www.sciencemag.org/content/351/6271/369/suppl/DC1
Materials and Methods
Figs. S1 to S15
Table S1
References (*39*–*41*)

14 October 2015; accepted 9 December 2015
10.1126/science.aad6378

GEOCHEMISTRY

Archean upper crust transition from mafic to felsic marks the onset of plate tectonics

Ming Tang,[1]* Kang Chen,[2,1] Roberta L. Rudnick[1]†

The Archean Eon witnessed the production of early continental crust, the emergence of life, and fundamental changes to the atmosphere. The nature of the first continental crust, which was the interface between the surface and deep Earth, has been obscured by the weathering, erosion, and tectonism that followed its formation. We used Ni/Co and Cr/Zn ratios in Archean terrigenous sedimentary rocks and Archean igneous/metaigneous rocks to track the bulk MgO composition of the Archean upper continental crust. This crust evolved from a highly mafic bulk composition before 3.0 billion years ago to a felsic bulk composition by 2.5 billion years ago. This compositional change was attended by a fivefold increase in the mass of the upper continental crust due to addition of granitic rocks, suggesting the onset of global plate tectonics at ~3.0 billion years ago.

Magnesium content (and its ratio to other elements) is commonly used as an index of igneous differentiation and melting conditions, which are responsible for much of the compositional variation seen in silicate rocks. Thus, MgO content serves as a first-order measure of silicate rock differentiation. Estimating the average MgO content in the upper continental crust, and from that the bulk composition of this crust is, however, challenging. There are two basic approaches to determine the composition of the upper continental crust (*1*–*3*): (i) weighted averages of surface rocks and (ii) average compositions of terrigneous sediments such as shales (*1*, *2*) and glacial diamictites (*4*) that naturally sample large areas of the upper continental crust. The surface rock method is compromised by sampling bias, which becomes increasingly critical with age, because erosion removes the upper continental crust with time, and ultramafic and mafic (magnesium- and iron-rich) rocks may be eroded faster than felsic (silica- and aluminum-rich) rocks (*1*). The terrigenous sediment method cannot provide robust average concentrations of soluble elements such as Mg, which are preferentially dissolved and transported to the oceans during chemical weathering (*5*).

We compiled geochemical data for Archean shales (including pelites and graywackes), glacial diamictites (*4*), and igneous rocks from 18 Archean cratons (*6*) to demonstrate that Ni/Co and Cr/Zn ratios provide relatively tight constraints on the MgO content in the Archean upper continental crust. We use the term "continental crust" here, although the nature of the crust that was emergent (i.e., exposed to weathering, and hence the generation of terrigenous sedimentary deposits) in the Archean may have been very different from the felsic crust that we know today (*7*).

First-row transition metal ratios Ni/Co and Cr/Zn show positive correlations with MgO content in igneous and metaigneous rocks from Archean cratons (Fig. 1) due to the differences in their partition coefficients between the crystallizing phases

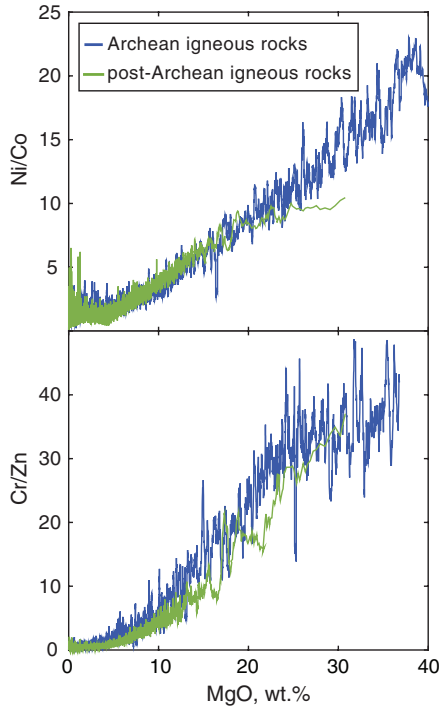

Fig. 1. Igneous Ni/Co-MgO and Cr/Zn-MgO differentiation trends for Archean and post-Archean rocks. We averaged every 20 samples to reduce scatter. Archean igneous trajectories are based on compiled igneous and metaigneous rocks from Archean cratons (*6*); post-Archean trajectories are plotted using compiled data from (*32*).

[1]Department of Geology, University of Maryland, College Park, MD 20742, USA. [2]State Key Laboratory of Geological Processes and Mineral Resources, School of Earth Sciences, China University of Geosciences, Wuhan 430074, China.
*Corresponding author. E-mail: tangmyes@gmail.com
†Present address: Department of Earth Science, University of California, Santa Barbara, CA 93106, USA.

and melts. In particular, Ni and Cr are more compatible than Co and Zn in fractionating phases [such as olivine, spinel, and pyroxenes (*8*–*10*)], making Ni/Co and Cr/Zn ratios sensitive to the earliest stages of igneous differentiation.

Ni, Co, Cr, and Zn are generally insoluble during chemical weathering (*2*), and their ratios should thus reflect the provenance of fine-grained terrigenous sedimentary rocks. The Ni/Co and Cr/Zn ratios show secular trends in sedimentary records (Fig. 2). Archean sedimentary rocks are characterized by high Ni/Co and Cr/Zn ratios, whereas post-Archean sedimentary rocks have much lower and relatively constant Ni/Co and Cr/Zn ratios. The average Ni/Co and Cr/Zn ratios in the latter (*11*) are consistent with estimates of the present-day upper continental crust composition derived from average loess and from large-scale surface sampling (Fig. 2). Cr can be oxidized to soluble Cr^{6+} in contact with present-day atmosphere (*12*). However, the low concentrations of Cr in present-day seawater [~4.0×10^{-9} mol/kg (*13*)], which hosts large amounts of soluble elements from the continents (~4.7×10^{-1} mol/kg of Na and ~5.3×10^{-2} mol/kg of Mg), does not support the idea that there was significant Cr loss from the upper crust due to oxidative weathering. In the anoxic Archean, Cr is expected to have been even less mobile. Lithology-sensitive weathering rates may potentially bias the composition of terrigenous sediments, but currently we don't see evidence for this effect on Ni/Co and Cr/Zn ratios (*6*). We thus conclude that there is limited fractionation between Ni and Co, or Cr and Zn, due to the processes that occur during weathering, erosion, sedimentation, and diagenesis.

The Ni/Co and Cr/Zn ratios in fine-grained terrigenous sedimentary rocks decrease with time within the Archean Eon, approaching the values of the present-day upper continental crust at the end of the Archean (Fig. 3). The decreasing Ni/Co and Cr/Zn ratios with time reflect progressively more felsic (lower MgO) upper continental crust from the Mesoarchean [3.5 to 3.0 billion years ago (Ga)] to the Neoarchean (3.0 to 2.5 Ga). The Ni/Co- and Cr/Zn-age correlations established for samples from many continents suggest that these systematics reflect global crustal evolution rather than regional phenomena.

We conducted a Monte Carlo mixing simulation to determine the average MgO content of the Archean upper crust (*6*), which we assumed was composed of rocks represented in the compiled Archean craton rock data set (n = 5063 for samples with complete SiO_2, MgO, Ni, Co, Cr, and Zn data), in order to match the average Ni/Co and Cr/Zn ratios recorded by the Archean sediments. The mixing scenarios that pass the Ni/Co and Cr/Zn filters yield the average MgO content for the Archean upper continental crust. Using this approach, we tracked the evolution of the MgO content in the Archean upper continental crust (Fig. 4) based on binned locality average Ni/Co

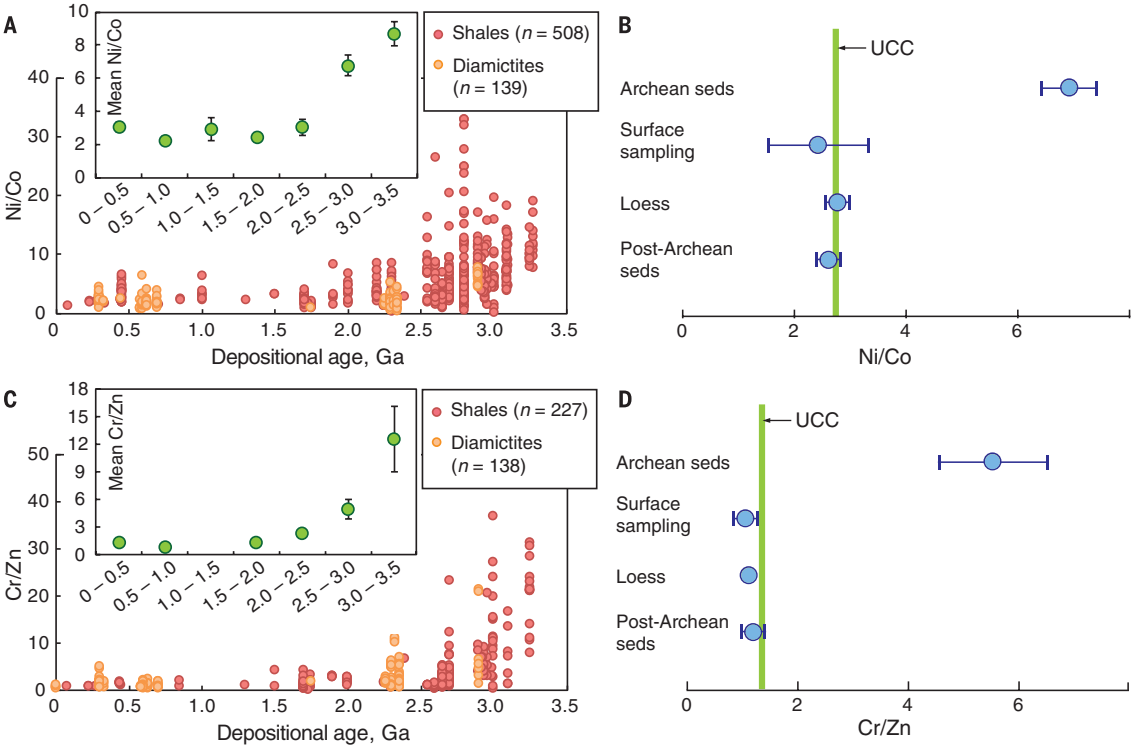

Fig. 2. Ni/Co and Cr/Zn ratios in terrigenous fine-grained sedimentary rocks (seds) through time [(A) and (C)] compared with the present-day upper continental crust [(B) and (D)]. Insets in (A) and (C) show age-binned Ni/Co and Cr/Zn ratios in terrigenous sediments (bin size = 0.5 Ga). Shale and diamictite data are provided in (*6*); loess data are from (*33*); and large-scale surface sampling data are from (*3*) and references therein. The green bars in (B) and (D) denote the reference values for present-day upper continental crust (UCC) (*3*). Error bars are 2 SE.

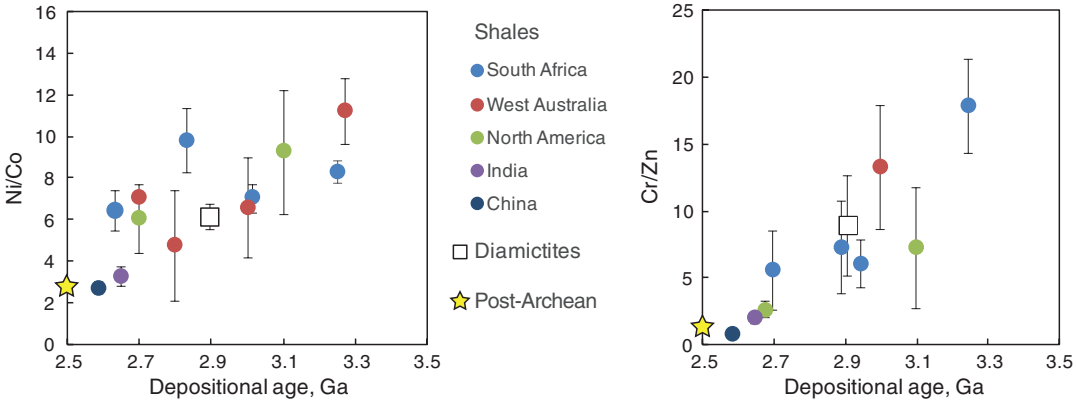

Fig. 3. Average Ni/Co and Cr/Zn ratios versus depositional ages in Archean fine-grained terrigneous sedimentary rocks from different localities. Data for individual samples were grouped by their localities (reflected by different colors) within 0.2-Ga bins. Error bars are 2 SE.

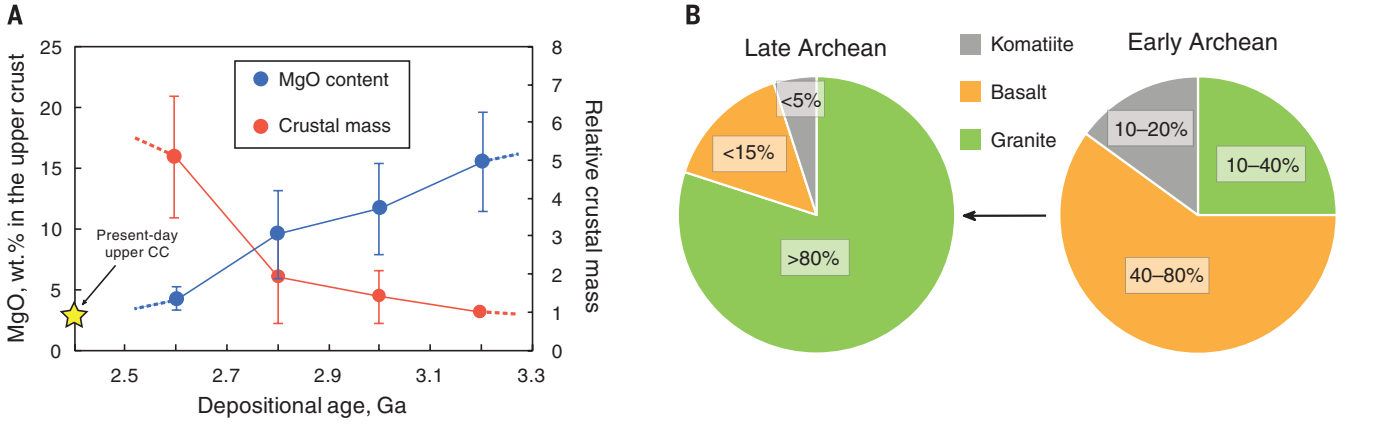

Fig. 4. Evolution of MgO content, relative mass (A), and the proportions of major rock types (B) of the upper continental crust in the Archean Eon. (A) MgO content was calculated based on the locality average Ni/Co and Cr/Zn ratios within each 0.2-Ga time interval, so that larger numbers of samples for particular localities do not have an undue influence on the outcome. Because the depositional ages of sedimentary rocks represent the minimum formation ages of the crust being sampled, both the MgO and upper crustal growth curves could shift toward older ages. Upper crustal masses are relative to that of the Mesoarchean upper continental crust. Error bars are 2 SD. (B) We calculated the proportions of TTGs, basalts, and komatiites, assuming that TTGs, basalts, and komatiites have average MgO contents of 1.4 wt % (*17*), 11 wt % (from compiled Archean craton samples with SiO_2 of 45 to 54%), and 30 wt % (*34*), respectively.

and Cr/Zn (Fig. 3). We found that the MgO content in the upper continental crust decreases from >11 weight % (wt %) in the Mesoarchean to ~4 wt %, at the end of the Archean, which is close to the present-day level of 2 to 3 wt % (*3*). The mafic upper continental crust in the early Archean was gradually replaced by a felsic upper continental crust in the Neoarchean and reached an average composition much like that of today around the Archean-Proterozoic boundary. The consistently low Ni/Co and Cr/Zn ratios in post-Archean sediments (Fig. 2) suggest a nearly constant composition for the upper continental crust since 2.5 Ga.

Although it has a high MgO content, the Archean upper continental crust may contain up to 40% tonalite-trondhjemite-granodiorites (TTGs) (Fig. 4). The budgets of incompatible elements in the sediments are controlled by the TTG components (yielding high La/Sm ratios), whereas transition metals (Ni, Co, Cr, and Zn) are controlled by mafic components.

Through most of the Archean, the upper continental crust had a mafic bulk composition (Fig. 4). This mafic composition, however, is not reflected in the mineralogy of Archean clastic sediments, which typically contain felsic minerals (e.g., detrital quartz, muscovite, and feldspar) (*14*). This disconnect between geochemical and mineralogical observations, as well as the low MgO contents in most Archean terrigenous sedimentary rocks (*15*), probably reflects preferential dissolution of mafic components (minerals and glasses) during chemical weathering (*6*). Minerals such as olivine weather congruently, releasing Mg, which is then transported to the ocean, where it may be sequestered into altered seafloor basalts through reverse weathering (*16*). Mafic to ultramafic volcanic glasses weather in a similar manner. In contrast to MgO, Ni, Co, Cr, and Zn may be incorporated into clay minerals or incorporated as metal-rich accessory phases after their release from the primary igneous phases.

We constructed a growth curve for the Archean upper continental crust based on MgO mass conservation. We assumed dilution of the upper continental crust MgO by addition of TTGs with an average of 1.4 wt % MgO (*17*). To make an upper continental crust with MgO of 4 wt % at the end of Archean requires the addition of a TTG mass that is four times that of the mafic upper continental crust older than 3.0 Ga (Fig. 4). Any addition of mafic igneous rocks to the upper continental crust would require even more felsic magma to balance the MgO content. Together, these observations suggest at least a fivefold mass increase of the upper crust in the Archean, with much of the felsic rocks being delivered in the Neoarchean. This inferred massive crustal growth in the Neoarchean is in line with certain crustal growth models (*2*, *18*) and corresponds to the peaks at ~2.7 Ga seen in both zircon U-Pb age (*18*, *19*) and mantle xenolith Re depletion age (*20*) spectra. Because our calculations are based on insoluble elements, the results are insensitive to weathering processes.

Such dramatic changes in the composition and mass of the upper continental crust suggest a profound and fundamental change in the processes that formed the Archean crust (Fig. 4). The rise of voluminous felsic magmatism that produced the TTGs, and the processes that formed the Archean TTGs, might have driven the evolution of the Archean crust. TTGs may be generated from both nonsubduction (the melting of mafic rocks in the lower crust) (*21*–*24*) and subduction (the melting of subducted plates) (*17*, *25*, *26*) origins. Melting and recycling of lower crustal mafic granulites might have persisted throughout the Archean Eon because of the high mantle temperature at that time (*27*). However, lower crust is generally depleted in water, which is important in the generation of granitic melts, including TTGs (*28*). It is thus doubtful that lower crustal melting, in the absence of subduction processes, would be efficient in producing such large amounts of TTGs that increased the mass of the Archean upper continental crust by a factor of 5. Assuming that Earth experienced a period of stagnant lid or drip tectonics before the onset of plate tectonics (*29*), the subaerial crust, which probably evolved from oceanic plateaus, had a total area of a fraction of the present-day continental crust and a composition dominated by basalt mixed with komatiites and minor TTGs generated by lower crustal melting. Approaching 3.0 Ga, the onset of global plate tectonics would have provided a continuous supply of water to the mafic source (such as subducted oceanic crust) that resulted in the rise of voluminous TTGs and other felsic magmas (*25*). Modern-style continental crust started to emerge, attended by extensive subduction in the Neoarchean. Substantially earlier global-scale plate tectonics (>3.5 Ga) are unlikely, considering the rapid mafic-felsic transition within the last 0.5 billion years of the Archean Eon. This timing is consistent with the constraints from diamonds from the subcontinental mantle (*30*), secular changes in Hf and O isotopes in zircon (*31*), and Rb-Sr systematics in magmatic records (*7*).

REFERENCES AND NOTES

1. K. C. Condie, *Chem. Geol.* **104**, 1–37 (1993).
2. S. R. Taylor, S. M. McLennan, *The Continental Crust* (Wiley, 1985).
3. R. L. Rudnick, S. Gao, 4.1 - Composition of the continental crust, in *Treatise on Geochemistry (Second Edition)*, H. D. Holland, K. K. Turekian, Eds. (Elsevier, Oxford, 2014), pp. 1–51.
4. R. M. Gaschnig *et al.*, *Earth Planet. Sci. Lett.* **408**, 87–99 (2014).
5. H. D. Holland, *The Chemical Evolution of the Atmosphere and Oceans* (Princeton Univ. Press, 1984).
6. Materials and methods are available as supplementary materials on *Science* Online.
7. B. Dhuime, A. Wuestefeld, C. J. Hawkesworth, *Nat. Geosci.* **8**, 552–555 (2015).
8. W. Leeman, K. Scheidegger, *Earth Planet. Sci. Lett.* **35**, 247–257 (1977).
9. I. Horn, S. F. Foley, S. E. Jackson, G. A. Jenner, *Chem. Geol.* **117**, 193–218 (1994).
10. H. Bougault, R. Hekinian, *Earth Planet. Sci. Lett.* **24**, 249–261 (1974).

11. In calculating the post-Archean average, we excluded data for Paleoproterozoic (2.5 to 2.0 Ga) sedimentary rocks, which might oversample the Archean upper crust and thus show slightly higher Ni/Co and Cr/Zn ratios.
12. R. Frei, C. Gaucher, S. W. Poulton, D. E. Canfield, *Nature* **461**, 250–253 (2009).
13. www.mbari.org/chemsensor/pteo.htm
14. S. M. McLennan, S. R. Taylor, A. Kröner, *Precambrian Res.* **22**, 93–124 (1983).
15. R. Feng, R. Kerrich, *Geochim. Cosmochim. Acta* **54**, 1061–1081 (1990).
16. P. Michalopoulos, R. C. Aller, *Science* **270**, 614–617 (1995).
17. H. Martin, J.-F. Moyen, *Geology* **30**, 319–322 (2002).
18. K. C. Condie, R. C. Aster, *Precambrian Res.* **180**, 227–236 (2010).
19. K. C. Condie, *Earth Planet. Sci. Lett.* **163**, 97–108 (1998).
20. D. G. Pearson, S. W. Parman, G. M. Nowell, *Nature* **449**, 202–205 (2007).
21. F. Albarède, *Tectonophysics* **296**, 1–14 (1998).
22. R. L. Rudnick, *Nature* **378**, 571–578 (1995).
23. R. H. Smithies, *Earth Planet. Sci. Lett.* **182**, 115–125 (2000).
24. J. H. Bédard, *Geochim. Cosmochim. Acta* **70**, 1188–1214 (2006).
25. S. Foley, M. Tiepolo, R. Vannucci, *Nature* **417**, 837–840 (2002).
26. R. P. Rapp, N. Shimizu, M. D. Norman, *Nature* **425**, 605–609 (2003).
27. T. E. Johnson, M. Brown, B. J. P. Kaus, J. A. VanTongeren, *Nat. Geosci.* **7**, 47–52 (2014).
28. N. T. Arndt, *Geochem. Perspect.* **2**, 405–533 (2013).
29. T. Gerya, *Gondwana Res.* **25**, 442–463 (2014).
30. S. B. Shirey, S. H. Richardson, *Science* **333**, 434–436 (2011).
31. B. Dhuime, C. J. Hawkesworth, P. A. Cawood, C. D. Storey, *Science* **335**, 1334–1336 (2012).
32. C. B. Keller, B. Schoene, M. Barboni, K. M. Samperton, J. M. Husson, *Nature* **523**, 301–307 (2015).
33. M. Tang, R. L. Rudnick, W. F. McDonough, R. M. Gaschnig, Y. Huang, *Geology* **43**, 703–706 (2015).
34. C. Herzberg *et al.*, *Geochem. Geophys. Geosyst.* **8**, Q02006 (2007).

ACKNOWLEDGMENTS

This project was supported by NSF grant EAR 0948549 and a Wylie Fellowship to M.T. We appreciate discussions with C. Hawkesworth, S. McLennan, K. Condie, N. Arndt, I. Puchtel, R. Gaschnig, D. Lowe, A. Hessler, and J. Hurowitz. We also thank three anonymous reviewers for their constructive comments. Geochemical data for the sedimentary rocks and Archean craton rocks (http://georoc.mpch-mainz.gwdg.de/georoc/) used in this work are available in the supplementary materials.

SUPPLEMENTARY MATERIALS

www.sciencemag.org/content/351/6271/372/suppl/DC1
Materials and Methods
Supplementary Text
Figs. S1 to S3
Databases S1 and S2
References (*35*–*38*)

29 September 2015; accepted 10 December 2015
10.1126/science.aad5513

COMPARATIVE BEHAVIOR

Oxytocin-dependent consolation behavior in rodents

J. P. Burkett,[1,2,3]* E. Andari,[1,2,3] Z. V. Johnson,[1,2,3] D. C. Curry,[2,3] F. B. M. de Waal,[2,3,4] L. J. Young[1,2,3,5]*

Consolation behavior toward distressed others is common in humans and great apes, yet our ability to explore the biological mechanisms underlying this behavior is limited by its apparent absence in laboratory animals. Here, we provide empirical evidence that a rodent species, the highly social and monogamous prairie vole (*Microtus ochrogaster*), greatly increases partner-directed grooming toward familiar conspecifics (but not strangers) that have experienced an unobserved stressor, providing social buffering. Prairie voles also match the fear response, anxiety-related behaviors, and corticosterone increase of the stressed cagemate, suggesting an empathy mechanism. Exposure to the stressed cagemate increases activity in the anterior cingulate cortex, and oxytocin receptor antagonist infused into this region abolishes the partner-directed response, showing conserved neural mechanisms between prairie vole and human.

Consolation, which entails comforting contact directed at a distressed party, is a common empathetic response in humans that emerges in the second year of life (*1*). Until now, consolation behavior has only been documented in a few nonhuman species and only in the context of naturally occurring aggressive conflicts, as first described in great apes (*2*, *3*) and subsequently in canids (*4*, *5*), corvids (*6*, *7*), and elephants (*8*). These observations have, so far, been taken to mean that consolation behavior may require advanced cognitive capacities (*9*). Nonetheless, rodents also manifest some of the empathy-related capacities (*10*–*16*) thought to underlie consolation in humans and chimpanzees (*1*, *17*). If consolation behavior were to be observed outside of species with advanced cognition, this would suggest that it rests on much older, more widespread, and less cognitive capacities and may be variably expressed because of species-specific evolutionary context. Moreover, observing consolation behavior in a laboratory rodent under reproducible conditions would allow for empirical research on causal biological mechanisms relevant to human mental health.

Rodents in the genus Microtus display diverse mating strategies and social structures. The prairie vole (*Microtus ochrogaster*) is a socially monogamous, biparental rodent species in which both males and females may participate in philopatric cooperative breeding in the parental nest (*18*). These social traits frequently coevolve with other cooperative or altruistic behaviors that increase direct or indirect fitness, including social buffering among colony members (*19*). In contrast, closely related meadow voles (*M. pennsylvanicus*) are promiscuous breeders with no formal social structure that show comparatively abbreviated, uniparental care of pups (*20*). We hypothesized that the prairie vole, but not the meadow vole, would show consolation behavior under reproducible laboratory conditions. Additionally, we hypothesized that as suggested for humans and great apes, consolation behavior in the prairie vole would be based on an empathy mechanism. Last, we hypothesized that consolation behavior would be mediated by conserved neurobiological and neurochemical mechanisms consistent with those implicated in empathy in humans.

Consolation behavior has been defined as an increase in affiliative contact in response to and directed toward a distressed individual, such as a victim of aggression, by an uninvolved bystander, which produces a calming effect (*2*). This definition emphasizes victims of aggression due to observational constraints in naturalistic studies. In humans, the definition includes individuals experiencing stress from other sources (*1*), a strategy used in elephants (*8*) and suggested for primates (*9*). On the basis of this research, we first developed a set of laboratory conditions under which unstressed male and female prairie voles ("observers") would respond spontaneously and selectively to stressed conspecifics ("demonstrators") with a prosocial, other-directed behavior (the "consolation test") (Fig. 1A). In this protocol, an observer and a demonstrator housed together are separated from each other, and the demonstrator either sits alone in a home cage compartment or is exposed to a stressor consisting of five tones paired with light foot-shocks (0.8 mA, 0.5 s) distributed over the course of 24 min (Pavlovian fear conditioning). The demonstrator is then reunited with the naïve observer, and the natural response is recorded and measured. Under these experimental conditions, licking and grooming directed by observers toward demonstrators (or "allogrooming") was significantly longer in duration (time-treatment interaction, $F_{1,11} = 6.7$, $P < 0.025$) and shorter in latency ($t_{11} = 3.9$, $P < 0.003$) after a separation during which the demonstrator was stressed (Fig. 1B and fig. S1). Prairie vole observers did not increase allogrooming toward demonstrators after a control separation, demonstrating the selectivity of the response. Both male and female observers

[1]Silvio O. Conte Center for Oxytocin and Social Cognition, Emory University, Atlanta, GA, USA. [2]Center for Translational Social Neuroscience, Emory University, Atlanta, GA, USA. [3]Yerkes National Primate Research Center, Emory University, Atlanta, GA, USA. [4]Utrecht University, Utrecht, Netherlands. [5]Department of Psychiatry, School of Medicine, Emory University, Atlanta, GA, USA.
*Corresponding author. E-mail: jpburke@emory.edu (J.P.B.); lyoun03@emory.edu (L.J.Y.)

Archean upper crust transition from mafic to felsic marks the onset of plate tectonics

Ming Tang, Kang Chen and Roberta L. Rudnick (January 21, 2016)
Science Translational Medicine **351** (6271), 372-375. [doi: 10.1126/science.aad5513]

Editor's Summary

New crustal clues from old rocks

The ghost of continental crust long eroded away may exist in certain element ratios found in Archean rocks. Tang *et al*. used Ni/Co and Cr/Zn ratios as a proxy for the magnesium oxide that long ago weathered away in Earth's oldest rocks. This allowed a reconstruction of rock composition, which appears to be very different from that of the crust today. The shift to contemporary crust composition occurred after the Archean era, suggesting the onset of plate tectonics.

Science, this issue p. 372

Science (print ISSN 0036-8075; online ISSN 1095-9203) is published weekly, except the last week in December, by the American Association for the Advancement of Science, 1200 New York Avenue NW, Washington, DC 20005.